Voltage-dependent Inactivation of T-Tubular Skeletal Calcium Channels in Planar Lipid Bilayers

RAFAEL MEJÍA-ALVAREZ, MICHAEL FILL, and ENRICO STEFANI

From the Department of Molecular Physiology and Biophysics, Baylor College of Medicine, Houston, Texas 77030

ABSTRACT Single-channel properties of dihydropyridine (DHP)-sensitive calcium channels isolated from transverse tubular (T-tube) membrane of skeletal muscle were explored. Single-channel activity was recorded in planar lipid bilayers after fusion of highly purified rabbit T-tube microsomes. Two populations of DHP-sensitive calcium channels were identified. One type of channel (noninactivating) was active (2 μM ± Bay K 8644) at steady-state membrane potentials and has been studied in other laboratories. The second type of channel (inactivating) was transiently activated during voltage pulses and had a very low open probability (P_o) at steady-state membrane potentials. Inactivating channel activity was observed in 47.3% of the experiments (n = 84 bilayers). The nonstationary kinetics of this channel was determined using a standard voltage pulse (HP = −50 mV, pulse to 0 mV). The time constant (τ) of channel activation was 23 ms. During the pulse, channel activity decayed (inactivated) with a τ of 3.7 s. Noninactivating single-channel activity was well described by a model with two open and two closed states. Inactivating channel activity was described by the same model with the addition of an inactivated state as proposed for cardiac muscle. The single-channel properties were compared with the kinetics of DHP-sensitive inward calcium currents (I_{Ca}) measured at the cellular level. Our results support the hypothesis that voltage-dependent inactivation of single DHP-sensitive channels contributes to the decay of I_{Ca}.

INTRODUCTION

Amphibian and mammalian skeletal muscle possess a dihydropyridine (DHP)-sensitive inward calcium current (I_{Ca}) (Beaty and Stefani, 1976; Stanfield, 1977; Chiarandini and Stefani, 1983; Donaldson and Beam, 1983; Lamb and Walsh, 1987), which is thought to be mediated by calcium channels present in the transverse tubular (T-tube) membrane (Nicola-Siri et al., 1980; Almers and Palade, 1981;

Address reprint requests to Dr. Enrico Stefani, Department of Molecular Physiology and Biophysics, Baylor College of Medicine, One Baylor Plaza, Houston, TX 77030.

Dr. R. Mejía-Alvarez is on leave from the Faculty of Medicine, Universidad Nacional Autónoma de México, Mexico City, Mexico.

J. GEN. PHYSIOL. © The Rockefeller University Press · 0022-1295/91/02/0393/20 $2.00
Volume 97 February 1991 393–412

Donaldson and Beam, 1983). This current has a slow (seconds) decay during depolarizing pulses under voltage clamp conditions. Three mechanisms have been proposed to explain the slow decay of this current: (*a*) Ca^{2+} depletion in the diffusion limited space of the T-tube lumen (Almers et al., 1981); (*b*) accumulation of Ca^{2+} in the myoplasm that could reduce Ca^{2+} driving force or induce Ca^{2+}-dependent inactivation (Brehm and Eckert, 1978; Tillotson, 1979); and (*c*) voltage-dependent inactivation at single-channel level (Sánchez and Stefani, 1983; Cota et al., 1984; Cota and Stefani, 1989; Francini and Stefani, 1989). In this study we explored these possibilities by examining the activation and inactivation properties of DHP-sensitive calcium channels from skeletal muscle T-tube membranes.

Due to morphological considerations, single DHP-sensitive channels from skeletal muscle T-tube cannot be studied in living muscle fiber. This channel has been studied using the lipid planar bilayer technique at steady-state membrane potentials (Coronado and Affolter, 1986; Ma and Coronado, 1988; Yatani et al., 1988). In this work we performed a comparative study of macroscopic calcium currents recorded in single muscle fibers and unitary currents from single calcium channels reconstituted in lipid planar bilayers.

We found that T-tube microsomes contain two populations of DHP-sensitive calcium channels. One type (noninactivating) is recognized by spontaneous activity at steady-state potentials and is identical to that studied elsewhere. The other type (inactivating) is transiently activated by depolarizing pulses. Inactivating channels open with a τ of 23 ms and slowly inactivate with a τ of 3.7 s. Since the rate of channel inactivation is comparable to the rate of I_{Ca} decay from isolated muscle fibers, we suggest that voltage-dependent inactivation at the single-channel level contributes to the decay. The reported channel kinetics were adequately described by a Markovian model that includes two closed, two open, and one inactivated state.

MATERIALS AND METHODS

Microsome Preparation

Skeletal muscle from the hind legs and back of New Zealand white rabbits (2–3 kg) was used to prepare microsomes as described in detail elsewhere (Hamilton et al., 1989). Briefly, the tissue (250 g) was minced and homogenized in a cold buffer (1:1 wt/vol) of 0.3 M sucrose and 20 mM Tris maleate (pH = 7.0). A cocktail of protease inhibitors (100 μM PMSF, 100 μM aminobenzamide, 1 μM pepstatin A, 1 μg/ml leupeptin, and 1 μg/ml aprotinin) was added and was present throughout the fractionation procedure. Homogenate was centrifuged (3,000 *g*, 30 min) and the supernatant (S1) was collected. The pellet was rehomogenized and centrifuged (3,000 *g*, 30 min) to obtain a second supernatant (S2). Supernatants (S1 and S2) were centrifuged (10,000 *g*, 30 min) separately and the pellets were discarded. KCl was added to both S1 and S2 supernatants to a final concentration of 0.5 M. The mixtures were stirred (1 h) and then centrifuged (100,000 *g*, 45 min). Each pellet was then hand-homogenized in 0.3 M sucrose, 0.4 M KCl, and 10 mM MOPS (pH = 7.4). These homogenates were sedimented (130,000 *g*, 14 h) through a discontinuous sucrose gradient. Microsome fractions were collected at the interfaces, pelleted (130,000 *g*, 30 min), and resuspended in 10% sucrose, 0.1 M KCl, and 5 mM PIPES (pH = 6.8). All microsome fractions were kept frozen (−80°C) until use in bilayer experiments.

Only the lightest fractions were used in these experiments. These microsomal fractions had substantial DHP binding ([^{3}H]PN200-110, 25–50 pM/mg, K_d = 0.5 nM) and low [^{3}H]ryanodine binding (0.4–0.9 pM/mg), indicating that these fractions were enriched in T-tube membrane (Hamilton et al., 1989). Using Coomassie brilliant blue SDS-PAGE analysis of the microsomal fractions, the subunits of the DHP receptor were separated and identified. The α_1 subunit was identified by molecular weight and by the fact that it is the only polypeptide in the T-tube membranes that is specifically labeled by the DHP, [^{3}H]azidopine (Hamilton et al., 1989). This is an important point, indicating that the microsomes used in our single-channel experiments contained only a single family of DHP-binding protein.

Single-Channel Recording

Planar lipid bilayers were painted across a 100-μm aperture in a Delrin cup using the Muller-Rudin technique. The lipid painting solution contained synthetic lipids (50 mg/ml, 1:1, palmitoyl-oleoyl-phosphatidyl-ethanolamine and palmitoyl-oleoyl-phosphatidyl serine) dissolved in decane. The side of the bilayer to which microsomes were added is referred to as *"cis."* The other side is referred to as *"trans."* Single-channel activity was recorded in the following solution (in mM): 50 NaCl, 10 Na-HEPES (pH = 7.0), 0.01 $CaCl_2$, and 0.0025 (±) Bay K 8644. The recording solutions in both chambers were the same at the beginning of the experiment. After the bilayer was formed, 100 mM $BaCl_2$ was added in the *cis* side as current carrier cation and to make the ionic gradient necessary to optimize vesicle-bilayer fusion. Membrane potentials are reported as *cis* potential (reference *trans*). All single-channel open events (upward deflections) represent Ba^{2+} moving *cis* to *trans*. As reported in the Results, the sidedness of reconstituted channels was determined by voltage dependence. Both channel orientations were equally probable. When channels were oriented with the cytoplasmic side facing *trans* chamber, single-channel current (Ba^{2+} moving *cis* to *trans*) is equivalent to macroscopic inward current (Ca^{2+} moving into the cell). All experiments were performed at room temperature.

Nonpolarizing electrodes (Ag/AgCl) connected each side of the bilayer to the amplifier via 50 mM NaCl agar bridges were used. The amplifier was designed to optimize the signal-to-noise ratio and provide capacity transient cancellation during pulses. A detailed diagram of the circuit is shown elsewhere (Hamilton et al., 1989). Continuous data were sampled at 3 kHz and stored on video tape. P-Clamp software (Fetchex or Clampex; Axon Instruments, Inc., Burlingame, CA) was used for data collection. The computer simultaneously sampled current (100 Hz) and provided command voltages to the bilayer through a 12-bit A/D-D/A converter. Single-channel records were filtered at 30–50 Hz by an 8-pole Bessel filter.

Single-Channel Data Analysis

Continuous data files were analyzed with a personal computer using a commercially available single-channel analysis program (Iproc 2.0; Axon Instruments, Inc.). Discontinuous data files (pulse experiments) were analyzed with custom-made software. To eliminate capacitative transients, blank sweeps were averaged, filtered, and subtracted from all other sweeps of the same file. Openings were detected by setting a detection threshold at 50% of the average open-channel amplitude (Colquhoun and Sigworth, 1983). Open time probabilities (P_o) were calculated from total amplitude histograms by fitting a sum of Gaussian distributions by a nonlinear, least squares method (Levenberg-Marquardt algorithm). Idealized data were corrected for dead time due to filter characteristics and sampling frequency (Colquhoun and Sigworth, 1983). Dwell time distributions were logarithmically binned and the probability density functions (pdf) were fitted by the maximum likelihood method (Sigworth and Sine, 1987; software provided by Dr. R. Latorre and Dr. O. Alvarez from the University of Chile,

Santiago, Chile). Our results could be described by a Markovian model containing two open and two closed states. The transition rate constants were calculated from the pdf parameters. To access the accuracy of the model single-channel simulation software (CSIM 2.0; Axon Instruments, Inc.) was used. Simulated and experimental data were processed in parallel and then compared.

Voltage Clamp Recording

Electrical recordings were performed on single cut fibers from the extensor digitorum longus muscle from Wistar rats using the double Vaseline-gap technique as described in detail elsewhere (Kovács et al., 1983; García and Stefani, 1987; Francini and Stefani, 1989). Briefly, a 1-cm fiber segment was dissected in a relaxing solution containing (in mM): 95 K_2SO_4, 10 $MgCl_2$, 0.4 $CaCl_2$, and 10 K-HEPES, pH = 7.2. The fiber segment was mounted in a plastic chamber in a solution containing (in mM): 150 K-glutamate, 2 $MgCl_2$, 1 K_2EGTA, and 10 K-HEPES, pH = 7.2. Using two vaseline seals, the center portion of the fiber segment was electrically isolated. The center compartment (bounded by the vaseline seals) contained extracellular solution (150 TEA-CH_3SO_3, 2 $CaCl_2$ 2 $MgCl_2$, 0.0025 (±) Bay K 8644, 1 3,4-diaminopyridine, 0.001 tetrodotoxin, and 5 TEA-HEPES, pH = 7.2), while the cut ends of the fiber segment were bathed in intracellular solution (120 Na-glutamate, 3 Mg-ATP, 5 Na_2-phosphocreatine, 10 Na_2-EGTA, 10 glucose, and 10 Na-HEPES, pH = 7.2). All solutions were adjusted to 300 mosM. The experiments were carried out at 21°C. An IBM-compatible AT personal computer was used for data acquisition (D/A-A/D conversion by Axolab-1; Axon Instruments, Inc.) and analysis (P-Clamp software; Axon Instruments, Inc.). Linear current components were digitally subtracted by scaled control currents obtained with small negative pulses of one-fourth test pulse amplitude. Electrical properties of the fibers and seals were measured following the procedures of Irving et al. (1987). Averaged data are presented as the mean ± SD.

RESULTS

The goal of this study was to compare current recordings at the cellular level with single-channel measurements of the DHP-sensitive calcium channel. The single-channel methodology requires the presence of the DHP agonist (±) Bay K 8644. Additionally, bilayer viability limits the holding potential to ±50 mV. Thus, whole-cell experiments were performed in the presence of (±) Bay K 8644 and from identical holding potentials.

I_{Ca} Kinetics at the Cellular Level

A recording of I_{Ca} from a rat fiber in the presence of 2.5 μM (±) Bay K 8644 is shown in Fig. 1 *A*. One of the principal characteristics of this inward current is its slow decay during depolarizing pulses. The possible involvement of outward current in the decay is unlikely since the decay of I_{Ca} followed the envelope of the tail current measurements (Fig. 1 *A*, 0.4–2.2-s traces are superimposed). The fiber was held at −50 mV and then stimulated by pulses to 0 mV with incrementing durations. Fig. 1 *B* shows the relationship between the maximum value of tail current amplitude and the pulse duration. I_{Ca} inactivates monoexponentially with a τ of 0.49 s (average τ = 0.6 ± 0.14 s, n = 4).

The time course of I_{Ca} in the presence of agonist (± Bay K 8644) can be described

by the following expression:

$$I_{Ca} = A[1 - \exp(-t/\tau_m)]^a[h_\infty - (h_\infty - 1)\exp(-t/\tau_h)]^b \quad (1)$$

where A is an amplitude factor, a and b are integer constants, and τ_m, τ_h, and h_∞ are the Hodgkin and Huxley parameters used to describe sodium currents in squid axons. Fig. 1 *C* shows a record of I_{Ca} elicited by a depolarizing pulse to 0 mV (HP = −50 mV). The experimental data (open circles) were well described by Eq. 1.

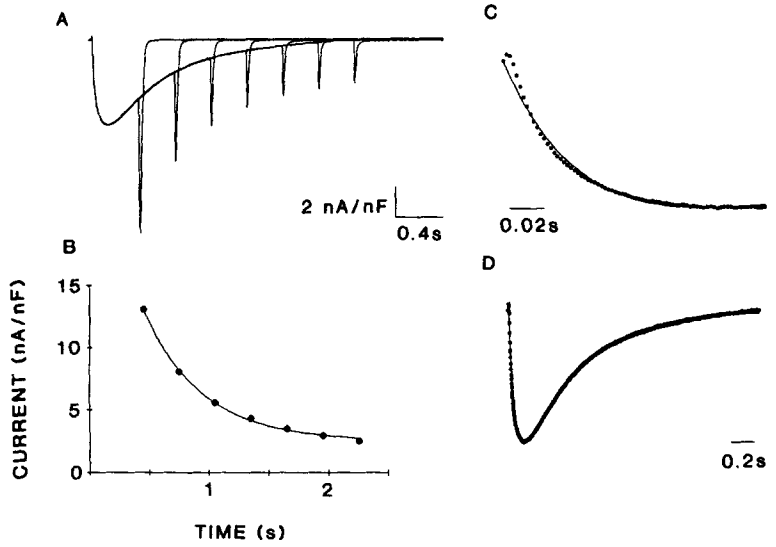

FIGURE 1. Transient slow inward I_{Ca} recorded in mammalian skeletal muscle cut fiber. (*A*) I_{Ca} records were elicited by single depolarizing pulses to 0 mV from −50 mV of HP. Seven traces of different duration are superimposed to show the reduction of the maximal amplitude of tail currents as an indicator of the current decay due to I_{Ca} inactivation. (*B*) The maximal amplitude of the tail current (*dots*) is plotted as function of the pulse duration. The continuous curve is a single exponential fitting to the experimental data with a τ = 0.49 s. (*C*) The longest trace from *A* has been displayed to show the activation phase of I_{Ca}. The open circles correspond to the experimental data, whereas the line is the theoretical description of the current based on the Hodgkin and Huxley model (Eq. 1): a = 1 and τ_m = 0.055 s. (*D*) The same trace at a different time scale to show the activation and inactivation components. The line is the best fit using Eq. 1, τ_h = 0.53 s.

The first points of the record are poorly fit since the initial outward charge movement was not considered. The best-fit I_{Ca} activation was obtained when τ_m was 55 ± 0.9 ms and a was 1.0 (continuous line). Expansion of the time scale (Fig. 1 *D*) reveals the inactivation component of I_{Ca}. The decay phase was best fit when b = 1.0 and τ_h = 527 ± 3.2 ms. This time constant of inactivation was practically identical to that obtained by the tail current analysis. These results in mammalian fibers, in agreement with previous work in frog skeletal muscle fibers, suggest that the I_{Ca} decay is due to

inactivation of I_{Ca} (Cota et al., 1984). We further investigated the inactivation properties of single DHP-sensitive calcium channels in bilayers using similar pulse protocols.

Single-Channel Activity under Stationary Conditions

Steady-state T-tube calcium channel activity at +20 mV (stationary conditions) is shown in Fig. 2 *A*. These records illustrate the high degree of complexity associated with this channel. Three amplitude levels and a wide range of open times are characteristic features of the DHP-sensitive calcium channel (Ma and Coronado, 1988; Yatani et al., 1988). Transitions between amplitude levels were frequently

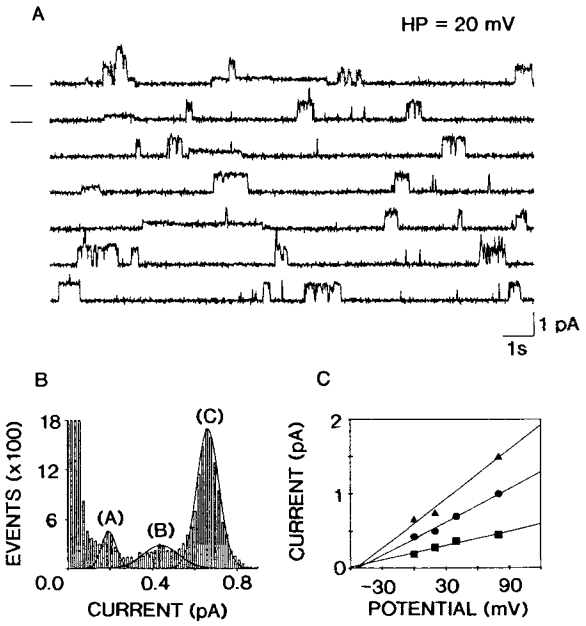

FIGURE 2. DHP-sensitive calcium channel activity recorded at steady potential. (*A*) Records obtained at 20 mV of holding potential in 100/0 (*cis/trans*) mM of $BaCl_2$ gradient. Openings are upward deflections; the baseline is indicated by the lines at the left of the two first rows. Data were filtered at 50 Hz. At least three single amplitude levels could be distinguished. (*B*) Total amplitude histogram from 20 min of continuous recording. The histogram contains the records shown in *A*. Three amplitude levels were resolved and fitted by Gaussian distributions. The values of the peaks were 0.19 ± 0.04 pA, 0.43 ± 0.09 pA, and 0.66 ± 0.05 pA. Open probabilities (A = 0.016; B = 0.023; C = 0.087) were calculated by comparison of areas. (*C*) Current–voltage relationship with three slope conductances (*triangles*, 11 pS; *circles*, 7 pS; and *squares*, 3 pS). Data are average of four experiments.

observed, mostly involving the two largest ones. Transitions involving the smallest state were rare. In contrast to the two largest amplitude levels, the smallest one typically had very long open times. Fig. 2 *B* shows a total amplitude histogram constructed from 20 min of continuous recording. Three clearly distinguishable amplitude peaks were identified. These peaks were fitted by Gaussian distributions. The mean of the distributions indicate open channel amplitudes of 0.19 ± 0.04, 0.43 ± 0.09, and 0.66 ± 0.05 pA. Comparison of individual areas to total area indicate that the smallest amplitude level had a P_o of 0.016. The intermediate and largest levels had P_o's of 0.023 and 0.087, respectively. The overall P_o was 0.126. The conductances of the three states were 3, 7, and 11 pS (Fig. 2 *C*).

Single-Channel Activity under Nonstationary Conditions

In addition to steady-state channel activity (Fig. 2), we also observed transient single-channel activity after a rapid change in holding potential (nonstationary conditions). In our initial observation (Fig. 3), a holding potential change from −50 mV to 0 mV (upward arrow) triggered channel activity, which spontaneously diminished with time. Returning the holding potential to −50 mV (downward arrow) did not trigger channel activity.

To study the nonstationary characteristics of this channel (inactivating channel), repetitive pulses were applied to the bilayer. Representative records from one such experiment are shown in Fig. 4. The P_o at steady-state potentials (0 and −50 mV,

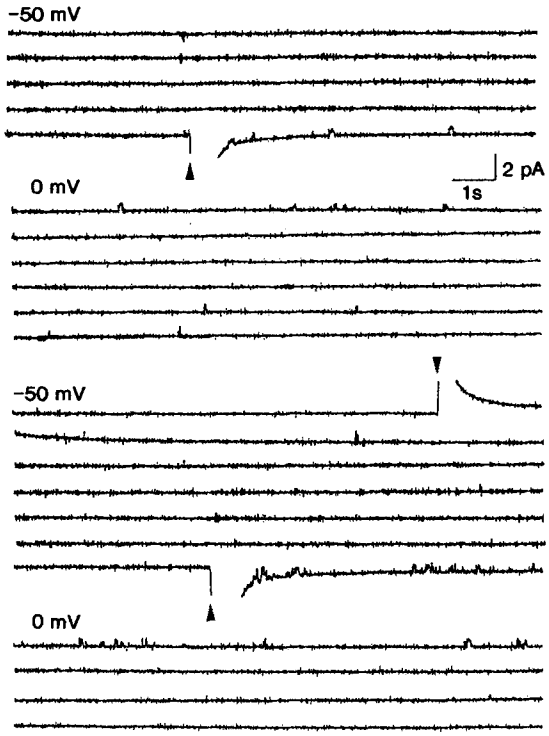

FIGURE 3. Initial observation of transient channel activity. All traces are from one continuous recording. The single-channel openings are upward deflections. Transient capacity current was not canceled. A change in the holding potential (indicated by arrows) transiently activates the channel. This phenomenon was observed each time we performed this maneuver.

data not shown) was very low. Channel activity was only observed by depolarizing the bilayer. During pulse experiments, channel activity was observed in nearly every sweep. Opening events were clustered at the beginning of the pulses. The frequency of activity was very low at the end of the pulses. The total amplitude histogram is plotted in Fig. 4 *B*. One amplitude peak was clearly resolved (0.5 pA) and fitted by a Gaussian distribution. A poorly resolved second peak (0.75 pA, dotted lines) is also shown. The main conductance of this channel was 9 pS (Fig. 4 *C*). The inactivating channel was observed in 40 bilayers (47.6%, $n = 84$).

To verify the identity of the inactivating channel, the effects of nitrendipine (10 μM), a DHP calcium channel antagonist, were explored. In noninactivating channels,

10 μM nitrendipine decreased the P_o from 0.09 ± 0.01 to 0.02 ± 0.01 ($n = 6$, $P < 0.01$) without altering current amplitude (data not shown). In the inactivating channels (Fig. 5), addition of nitrendipine (10 μM) decreased the P_o from 0.18 ± 0.06 to 0.02 ± 0.01 ($n = 6$, $P < 0.01$). This result indicates that both the noninactivating and inactivating channels are DHP sensitive.

The voltage dependence of the channel allowed us to determine the sidedness of the reconstituted channel. Frequently, inactivating channels were not activated by the standard pulse (−50 to 0 mV). In these instances, channel activity was triggered by the opposite pulse (+50 to 0 mV). Thus, microsome–bilayer fusion can result in channels oriented in either direction as was predicted by [^{3}H]ouabain binding experiments performed on these microsomes. Binding experiments indicated that

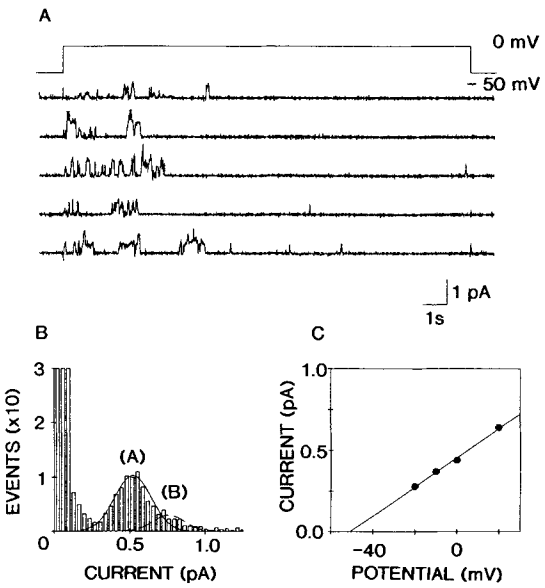

FIGURE 4. Voltage-dependent inactivating channel during pulses. (*A*) Channel activity elicited by pulsing the bilayer to 0 mV from −50 mV of holding potential; the interval between pulses was 18 s; linear leak and capacity current were eliminated by subtracting an average record of null traces. (*B*) Amplitude histogram constructed with all the points recorded during the pulse. The P_o of each peak ($A = 0.017$; $B = 0.005$) was obtained by comparison of the distribution areas; it represents the average value through the pulse. (*C*) The current–voltage relationship of the main amplitude is plotted (9 pS).

the proportion of inside-out to outside-out microsomes was 1:1 (Hamilton et al., 1989). Channels oriented in both directions had similar single-channel kinetics and steady-state properties.

The same pulse protocols, as in Fig. 4, were applied to bilayers containing noninactivating channel activity. These experiments are shown in Fig. 6. Channel activity was observed in nearly every sweep. The frequency of opening events did not change during the pulse. Noninactivating channel activity was present in both polarized and depolarized conditions. The P_o, however, was significantly higher at 0 mV than at −50 mV. The total amplitude histogram (Fig. 6 *B*) shows three distinct amplitude levels. The slope conductances were 3, 7, and 11 pS (Fig. 6 *C*). These values are identical to those described under stationary conditions (Fig. 2 *C*).

Derivation of Macroscopic Parameters

The inactivating channel activity during depolarizing pulses rapidly increases (activates) to a peak and then slowly decays (inactivates). To derive the macroscopic parameters (activation and inactivation τ's) associated with this channel, sweeps from several experiments were combined to generate a sum current (HP −50 mV, pulse to 0 mV, 147 sweeps, 6 bilayers). The P_o was calculated from the sum current using the expression $I_s = P_o \cdot N \cdot i$, where I_s is the sum current, N is the total number of channels present in the bilayer, and i is the amplitude of single-channel current. The high P_o (0.25–0.50) at the beginning of the pulse allowed us to estimate N by the

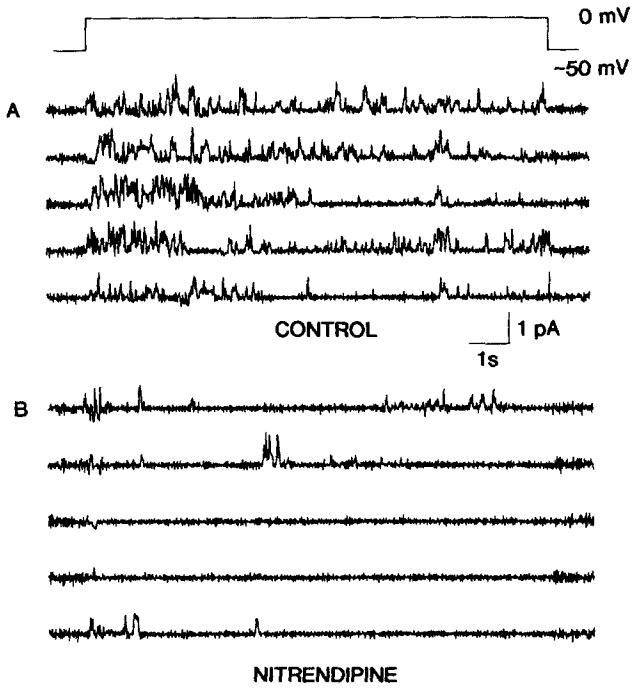

FIGURE 5. Nitrendipine effect on the inactivating channel. (*A*) Control record obtained with pulses from −50 mV to 0 mV. (*B*) After addition of nitrendipine at 10 μM symmetrical.

number of overlapped opening events (Fig. 7 *A*). The noise level in the sum current record (unfiltered) is dependent on the number of sweeps per trial. In our bilayer experiments the number of sweeps was limited by bilayer viability. The sum current shows a slow decaying phase (Fig. 7 *A*) which was fitted by a single exponential curve with a τ of 3.7 s (solid curve). The expansion of the time base in Fig. 7 *B* reveals that the sum current has a fast activation component. This component was fitted by a single exponential with $\tau = 23 \pm 1$ ms (solid curve).

Following the same procedure, a sum current record was generated from noninactivating channel experiments (Fig. 7 *C*). The single-channel current was elicited with the same pulse protocol (112 sweeps and 5 bilayers). The P_o during the pulse was

similar to the P_o measured at steady state (0.12). The channel activity did not display any decay or inactivation, and a fast activation component was observed (Fig. 7 *D*). This component was fitted by a single exponential with τ = 13 ms (solid curve). In summary, the two types of channel activities can be clearly distinguished by comparing the time course of the P_o's during a depolarizing pulse.

Dwell Time Data

In calcium channels without DHP agonists the frequency histogram of the open times can be described by a single exponential distribution (Brown et al., 1982; Fenwick et

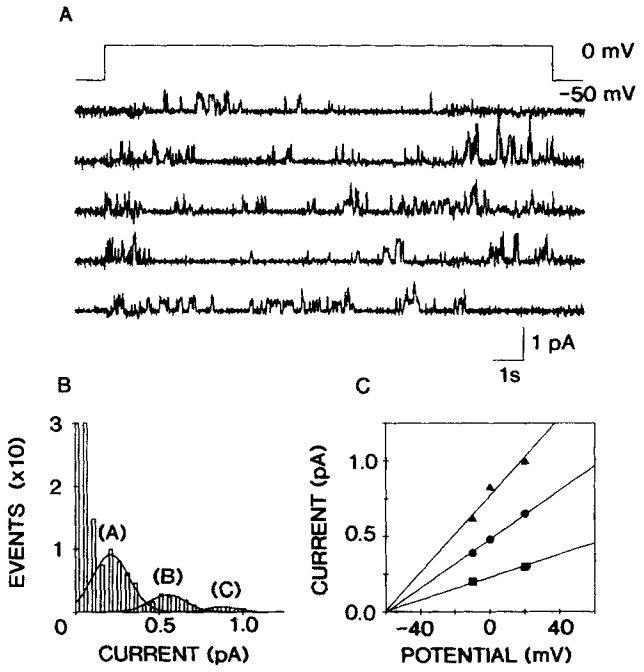

FIGURE 6. Noninactivating channel during pulses. (*A*) Some records obtained by pulsing the bilayer to 0 mV from a holding potential of −50 mV are displayed. We canceled the linear leak and capacity current with the same procedure as in Fig. 3. (*B*) The total amplitude histogram clearly shows three peaks that were resolved and fitted by Gaussian distributions. The open probabilities (A = 0.012; B = 0.007; C = 0.004) were obtained by comparison of areas. (*C*) The *I-V* relationship of this channel activity is plotted (*triangles*, 11 pS; *circles*, 7 pS; and *squares*, 3 pS).

al., 1982; Coronado and Affolter, 1986). In contrast, in the presence of DHP agonist, the open time histogram is described by the sum of two exponentials (Hess et al., 1984; Sanguinetti et al., 1986; Coronado and Affolter, 1986). In our experiments, the open time histograms of inactivating and noninactivating channels in the presence of the DHP racemic agonist (± Bay K 8644 2.5 μM symmetrical) were adequately described by the sum of two distributions (Fig. 8, upper histograms). The parameters of the pdf calculated by the maximum likelihood method (Table I) were equivalent in

both types of channels (inactivating τ's = 20 and 138 ms, noninactivating τ's = 20 and 123 ms). The closed-time frequency histograms (Fig. 8, bottom histograms) were also described by the sum of two exponential distributions (inactivating τ's = 20 and 459 ms, noninactivating τ's = 25 and 391 ms). The presence of two closed states was consistent with first latency histograms obtained from the same data. The first latency histograms had two waiting times with similar values of τ (data not shown). Close examination of the records (see Figs. 2–6) indicates that bursting kinetics are present in the DHP-sensitive channel. This observation was confirmed by the relative frequencies of the two short and two long events (Blatz and Magleby, 1989).

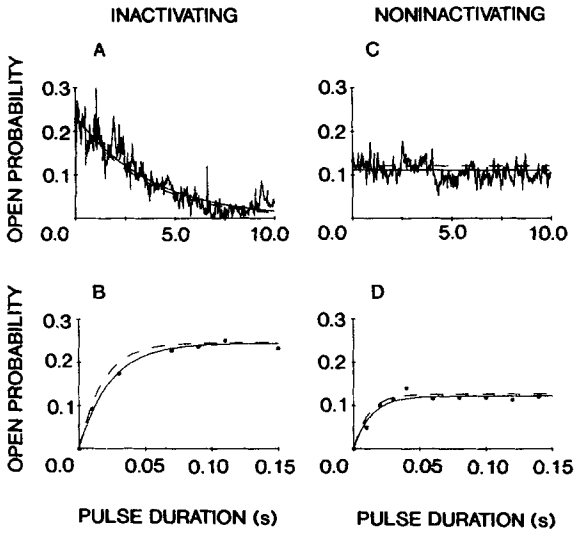

FIGURE 7. Rate of channel inactivation and activation. Individual records obtained from pulsing experiments were averaged and corrected by $I_s/N \cdot i$ factor (see text). The result (P_o) was plotted as function of pulse duration. (*A*) The P_o observed in inactivating channel is plotted (147 episodes from 6 bilayers). The decay of activity was fit by a single exponential curve (*solid line*) with a time constant of 3.7 s (the model prediction was 3.4 s; *dotted lines*). (*B*) The same data (*filled circles*) were replotted with a different time scale to resolve the very fast activation at the beginning of the pulse. The data were well fitted by a single exponential (*solid line*) with time constant of 23 ms. The model prediction was 18 ms. (*C* and *D*) Same type of analysis performed on the noninactivating channel (112 episodes from 4 bilayers). The activation (*D*) was fitted with a single exponential curve with a time constant of 13 ms (the model prediction was 11 ms; *dotted lines*). All the fitting curves were obtained by the nonlinear least-squares method.

Steady-State Kinetics at the Single-Channel Level

To further correlate single-channel properties to macroscopic observations, the voltage dependence of steady-state activation and inactivation of single DHP-sensitive calcium channels was explored (Fig. 9). To examine voltage dependence of inactivation (Fig. 9 *A*) a long depolarizing prepulse (10 s) to indicated potentials (at right) was used. The pulse potential was 0 mV. To examine the voltage dependence of activation (Fig. 9 *B*) the bilayer was held at −70 mV and depolarizing pulses (4 s) were delivered to indicated potentials. In both cases the degree of channel activity (P_o) was determined during the first second of the pulse. The relationships between P_o and membrane potential for activation and inactivation were well fit by a single

Boltzmann distribution (Fig. 9 *C*). The inactivation curve (open circles) was fit with $V_{1/2}$ = −32.6 mV and k = 7.4 mV ($V_{1/2}$ is midpoint, k is steepness factor). The activation curve (filled circles) was fit with $V_{1/2}$ = −37.3 mV and k = 5.1 mV.

Steady-State Kinetics at the Cellular Level

Voltage-dependent kinetics of I_{Ca} at steady-state conditions were examined at the cellular level in cut fiber experiments. To explore the steady-state inactivation a double-pulse protocol was used (Fig. 10 *A*). A conditioning pulse (10 s) to different membrane potentials was followed by a test pulse (0.1 s) to 0 mV. Prepulse potential is indicated at left of each trace. The effect of conditioning pulses on peak current was used to assess the degree of steady-state inactivation. Open circles in Fig. 10 *C* illustrate the fraction of Ca^{2+} channels that are not inactivated as function of the

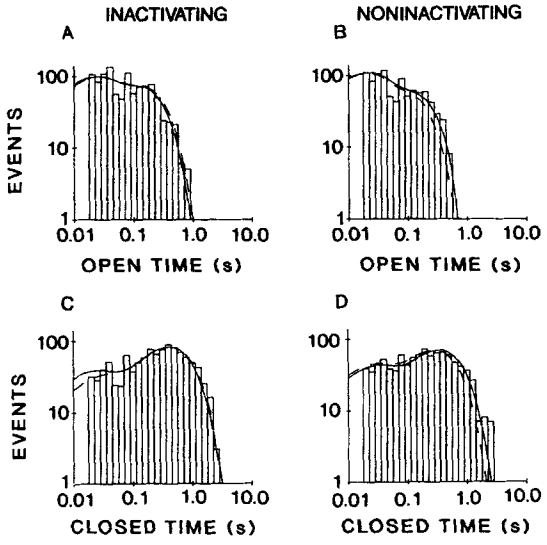

FIGURE 8. Open and closed time histogram distributions were plotted on a log–log scale from both inactivating and noninactivating channels. Fitting curves were obtained by the maximum likelihood method. Minimum time was limited by the sampling frequency (10 ms). (*A*) Open time histogram from an inactivating channel. Two exponential distributions were resolved and fit (*solid lines*). Probability density functions predicted by the model are superimposed (*dashed lines*). (*B*) Open time histogram from a noninactivating channel. (*C*) Closed time histogram from an inactivating channel. (*D*) Closed time histogram from a noninactivating channel.

conditioning pulse potential. The inactivation parameter (h_∞) was calculated as the ratio of peak currents with and without the conditioning pulse. The fit curve (Fig. 10 *C*) is described by the following expression:

$$h_\infty = 1/\{1 + \exp[(E - V_{h1/2})/k_h]\} \quad (2)$$

where E is the conditioning pulse potential, $V_{h1/2}$ is the midpoint, and k_h is the steepness factor (Hodgkin and Huxley, 1952). The data were best fit when V_h = −48 mV and k_h = 6.4 mV.

To explore steady-state activation, single depolarizing pulses to different test potentials were used. Representative records are shown in Fig. 9 *B*. Test potentials are indicated at the left of each trace. I_{Ca} becomes evident between −40 and −30 mV, reaching a maximal amplitude at ~10 mV. The peak I_{Ca} amplitude at 10 mV −2.7

$\mu A/cm^2$. To estimate the activation parameter (m_∞), the calcium permeability was calculated using the Goldman-Hodgkin-Katz equation:

$$P_{Ca} = \frac{I_{Ca}}{[(4F^2E)/(RT)]\left\{\frac{[Ca]_o[\exp(2F(E - E_{Ca})/RT) - 1]}{[\exp(2FE/RT)]}\right\}} \quad (3)$$

where F, R, and T have the usual thermodynamic meanings, $E_{Ca} = +150$ mV, and P_{Ca} is Ca^{2+} permeability. To account for the voltage dependence of I_{Ca} activation, P_{Ca} is expressed as:

$$P_{Ca} = P_{Ca} m_\infty \quad (4)$$

where P_{Ca} is the maximal Ca^{2+} permeability. The steady-state activation of I_{Ca} is shown in Fig. 10 *C* (filled circles). The fit curve was described by the following

TABLE I

Parameters of Dwell Time Frequency Distributions

State	Noninactivating channel		Inactivating channel	
	τ	Relative area	τ	Relative area
	ms		*ms*	
o_1	20 ± 2	0.6 ± 0.023	20 ± 3	0.5 ± 0.004
	(18 ± 7)	(0.6 ± 0.009)	(22 ± 1)	(0.5 ± 0.180)
o_2	123 ± 5	0.4 ± 0.023	138 ± 6	0.5 ± 0.004
	(100 ± 2)	(0.4 ± 0.009)	(150 ± 3)	(0.5 ± 180)
c_1	25 ± 6	0.29 ± 0.018	20 ± 3	0.25 ± 0.004
	(23 ± 2)	(0.3 ± 0.150)	(25 ± 12)	(0.19 ± 0.020)
c_2	391 ± 13	0.71 ± 0.018	459 ± 15	0.75 ± 0.004
	(321 ± 1)	(0.70 ± 0.150)	(479 ± 23)	(0.81 ± 0.020)

The values predicted by the model are shown in parentheses. Every value is shown ± SD. o_1 and o_2 are fast and slow open states, respectively; c_1 and c_2 are fast and slow closed states, respectively.

expression:

$$P_{Ca} m_\infty = P_{Ca}\{1 + \exp[(V_{m1/2} - E)/k_m]\}^{-1} \quad (5)$$

where $V_{m1/2}$ is midpoint, E is test pulse potential, and k_m is the steepness factor. Experimental data points were best fit when $V_{m1/2} = -11.5$ mV and $k_m = 7$ mV. The value of P_{Ca} was 1.06×10^{-6} cm/s.

DISCUSSION

In skeletal muscle T-tube membrane, two types of calcium channels have been identified on the basis of macroscopic current properties (Cota and Stefani, 1986; García et al., 1988). The L-type channel is characterized by its DHP sensitivity, high activation threshold, and slow inactivation. The other channel is not DHP sensitive. Since our bilayer experiments have identified two types of single-channel activity, it is

possible that these represent the two types of macroscopic Ca^{2+} currents. The two types of channels we describe here share many single-channel properties: (*a*) main conductance; (*b*) number of kinetic states; (*c*) burst behavior; and (*d*) DHP sensitivity. We believe, therefore, that both inactivating and noninactivating channel activities correspond to the L-type calcium channel.

L-type calcium currents, in single mammalian muscle fibers, fully inactivate with depolarization. Thus, the finding that in bilayer experiments one population of channels does not inactivate may suggest that during the membrane fractionation process some DHP-sensitive calcium channels lose the inactivating gate. This is not

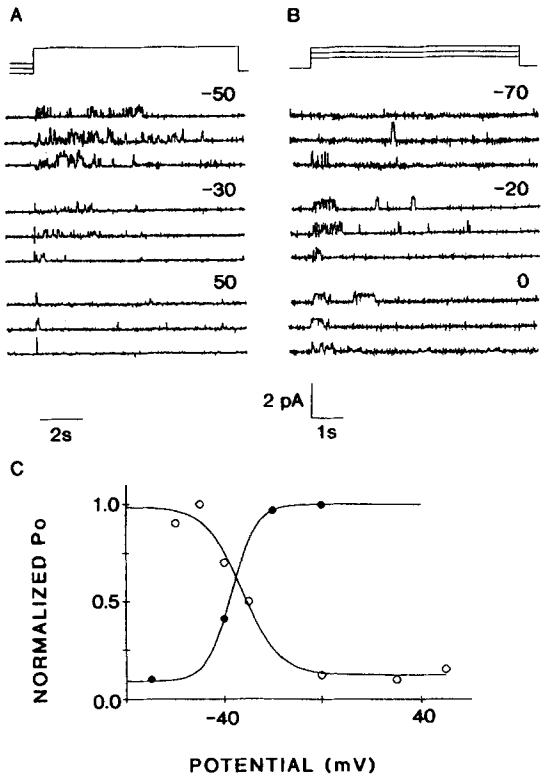

FIGURE 9. Steady-state kinetics of the inactivating channel. (*A*) Inactivation of channel activity by varying the holding potential to the indicated values. The test potential was 0 mV. (*B*) Activation of channel activity by increasing the test potential to the indicated values. The holding potential was −70 mV. (*C*) Activation and inactivation curves were generated by measuring the P_o (normalized to the maximum) during the first second of the pulse; the P_o was plotted as function of the membrane potential. The data were well fit by Boltzmann distributions. The activation curve was defined by the following parameters: V_m = −37 mV and k = 5.5. The inactivation curve was defined by V_m = −32.6 mV and k = 7.4.

unreasonable since Na channels lose the inactivation gate after a mild internal proteolysis (Armstrong et al., 1973).

Single-Channel Activity under Stationary Conditions

Noninactivating channel activity was monitored at stationary conditions over a wide range of holding potentials (±50 mV, limited by bilayer viability). In the absence of DHP agonists, we found an extremely low P_o (<0.001) and very fast kinetics (data not shown). In the presence of 2.5 μM racemic Bay K 8644, the steady-state P_o (HP = 0 mV) was ~0.1. Three conductance levels were identified (3, 7, and 11 pS). Thus,

the noninactivating channel recorded in these conditions was consistent with the results of several laboratories (Coronado and Affolter, 1986; Ma and Coronado, 1988; Yatani et al., 1988) concerning: (*a*) multiple conductance levels; (*b*) DHP sensitivity; and (*c*) main conductance near 11 pS (100 mM $BaCl_2$ *cis*). One difference between our observations and those of others concerns the relative mean lifetimes of the three conductance levels. We report here that the smallest conductance level has the longest mean lifetime, while Ma and Coronado (1988) have reported that the largest conductance level had the longest mean lifetime. Multiple substates with heterogeneity in mean lifetime reflects the complexity involved in analysis of single calcium channel records.

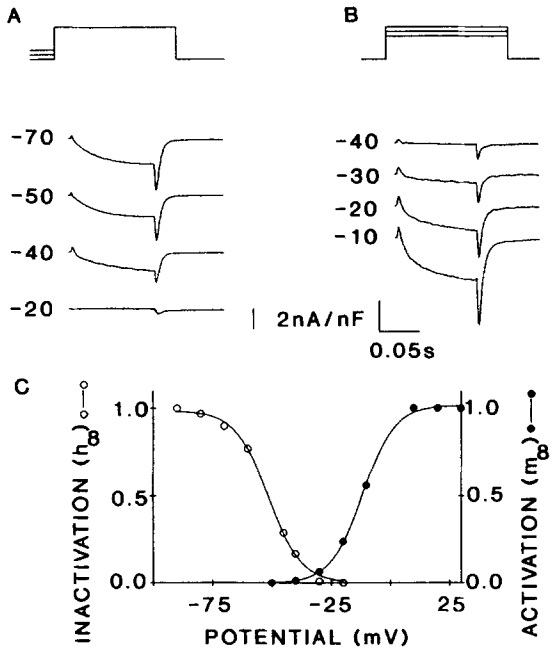

FIGURE 10. Steady-state kinetics of I_{Ca} at the cellular level. (*A*) Inactivation protocol: pulses to 0 mV (test potential) from different holding potentials. Representative traces are shown to illustrate the effect of conditioning pulse potential on the peak amplitude current during the test pulse. The prepulse holding potential is indicated with the numbers at the left of each trace. (*B*) Activation protocol from −50 mV of HP. The amplitude of the test potential is modified to activate different number of channels. Some records obtained with this protocol are presented. The number at the left of each record indicates the test potential. (*C*) The I_{Ca} steady-state kinetics of activation (m_∞) and inactivation (h_∞) were measured and plotted as a function of membrane potential. For the inactivation (*open circles*) the curve was defined by $V_{h1/2}$ = −48 mV and k_h = 6.5 mV. For the activation (*filled circles*) the curve was described by $V_{m1/2}$ = −11.5 mV and k_m = 7 mV.

Channel Activity under Nonstationary Conditions

In single fibers, the kinetics of I_{Ca} are voltage dependent. At the single-channel level, burst frequency and steady-state P_o of noninactivating channels are voltage dependent (Coronado and Affolter, 1986). These single-channel properties, however, cannot explain the characteristic decay of I_{Ca}.

The nonstationary kinetics of single L-type DHP-sensitive calcium channels in planar bilayers has recently been described in cardiac muscle (Rosenberg et al., 1988). We report here a similar description of DHP-sensitive calcium channels from

skeletal muscle. We have shown that T-tube microsomal fractions contain a population of DHP-sensitive channels that are transiently activated by sudden changes in holding potential. This transient activity is observed as a rapid rise and slow exponential decay of P_o. We have observed this phenomenon in ~50% of channel reconstitutions from six different membrane preparations from rabbit and rat skeletal muscle (rat data not shown). In most of our channel reconstitutions we observed one channel per fusing vesicle. In cases where multiple channels were incorporated it is possible that both inactivating and noninactivating channels were present simultaneously. When performing a steady-state experiment, all inactivating channels would be inactivated. When performing a pulsing experiment, the presence of noninactivating channels may explain why the sum current trace (Fig. 7) does not go to zero at long times. Similarities between the inactivating and noninactivating channels include: (*a*) identical open and closed states; (*b*) multiple conducting substates; (*c*) identical main conductances; and (*d*) blockade by 10 μM nitrendipine. The only distinguishing feature was that inactivating channels displayed inactivation.

Channel activation. In our single-channel experiments, the steady-state P_o at the holding potential (−50 mV) was significantly lower than the P_o at the test potential (0 mV). Thus, the observed activation at the single-channel level may reflect a redistribution in steady-state P_o after a voltage step. The activation (P_o) of a simple (one open/one closed state) voltage-dependent channel is theoretically described by a single exponential with the time constant dependent on the test potential. More complex schemes (e.g., multiple interconnected closed states) typically introduces a sigmoidal activation behavior. The single-channel activation data were well described by a single exponential. This was somewhat surprising since the proposed model contained more than one closed state. Thus, the measured activation phenomenon either (*a*) is limited by the resolution of our recording system, (*b*) is dependent on only one closed state, or (*c*) is dependent on linearly connected multiple closed states. Regardless of the theoretical interpretation, the time constant of the exponential fit roughly represents the half-time of activation.

In single fibers the slow Ca^{2+} current is transiently activated during depolarizing pulses. The activation phase was fit by a single exponential with a τ of 55 ± 1 ms (five fibers). At the single-channel level, the activation time constant triggered by the standard pulse (−50 to 0 mV) was 23 ± 3 ms. Direct comparison of single-channel data and cut fiber results, however, is difficult since experimental conditions are not identical. Nevertheless, the activation rate of single channels in the bilayer is adequately fast to account for I_{Ca} activation at the cellular level. The steady-state activation curve at the single-channel level is shifted by ~25 mV compared with the same curve in whole-cell experiments. The difference in the current carrier (Ca^{2+} for cut fiber, Ba^{2+} for bilayer) or in its concentration cannot account for this shift (cf. Fig. 4 in Cota and Stefani, 1984). The origin of this dissimilarity is unknown, but may arise from the different composition of native T-membrane and the artificial bilayer.

Channel inactivation. The principle observation in our work is the voltage-dependent inactivation of single DHP-sensitive calcium channels. This decay in P_o cannot be explained by redistribution of steady-state P_o (see activation discussion above). The decay in P_o was fit by a single exponential with τ = 3.7 ± 0.06 s (six

bilayers). Our hypothesis is that voltage-dependent inactivation at the single-channel level may contribute to the decay in I_{Ca} ($\tau = 0.6 \pm 0.13$ s, five fibers) observed at the cellular level. Decay of I_{Ca} may arise from one or more of the following mechanisms: (*a*) calcium depletion in the T-tube lumen (Almers et al., 1981); (*b*) internal calcium accumulation and/or calcium-induced inactivation of the channel (Brehm and Eckert, 1978; Tillotson, 1979); and (*c*) voltage- and time-dependent inactivation of channel activity (Cota et al., 1984; Francini and Stefani, 1989). Although single DHP-sensitive channels inactivate in a voltage-dependent way, our data do not exclude the other mechanisms.

The role of calcium-induced inactivation of the channel is indirectly addressed by our bilayer experimental methodology. Single channels were fused and monitored in the presence of barium gradient (100/0 mM). It is possible that as barium passes through the channel it binds to a site on the myoplasmic face of the channel, causing inactivation (Tillotson, 1979). Our observation that channels inactivate regardless of channel orientation is not consistent with a divalent induced inactivation mechanism. Since 100 mM barium is present only on one side of the bilayer (*cis*), a barium-induced mechanism would predict that inactivation would only be observed in channels oriented with the myoplasmic surface on the low barium side of the bilayer.

The role of the depletion mechanism in the decay of I_{Ca} cannot be addressed at the single-channel level. The small diffusion-limited space of a T-tube cannot be artificially duplicated in the bilayer system. In our experiments, depletion of current carrier was negligible due to the large volume (3 ml) of our experimental chambers. In summary, our results support the possibility that a voltage-dependent inactivation process at the single-channel level may contribute to the decay observed in I_{Ca} recorded in cut fiber experiments.

Markovian Models of Channel Activity

The model used to explain the nonmodal gating of DHP-sensitive calcium channels from cardiac muscle (Lacerda and Brown, 1989) was used to describe the kinetics of the channels we describe in skeletal muscle. The model includes four closed, two open, and one inactivated state. The Lacerda and Brown (1989) model includes four closed states to account for DHP-free and DHP-bound conditions. Since all our experiments were performed in saturating levels of DHP, we only considered the two DHP-bound closed states. The model used to fit our data (Scheme 1) includes two open (O_1 and O_2) and two closed states (C_1 and C_2). These states have either short (O_1 and C_1) or long (O_2 and C_2) mean dwell times. The model also included an inactivated state. This state was omitted from model considerations of noninactivating channel activity. The initial transition rates matrix (Colquhoun and Hawkes, 1982) was constructed using the pdf parameters obtained from our experimental data. The matrix input was slightly adjusted until simulated channel data generated from the model were adequately fitted by the experimental pdf. The model predictions for closed and open times are shown in Figs. 7 and 8 with dotted lines. The transition rate constants are shown in Scheme 1.

In summary, our experimental results and kinetics modeling reveal that: (*a*) T-tube microsomes contain two types of DHP-sensitive calcium channel activity; (*b*) the two

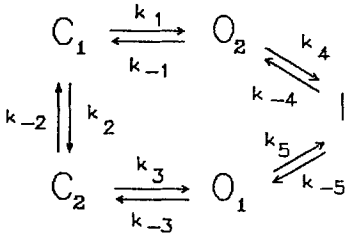

$k_1 = 38.5\ s^{-1}$
$k_{-1} = 7.0\ s^{-1}$
$k_2 = 3.5\ s^{-1}$
$k_{-2} = 0.2\ s^{-1}$
$k_3 = 2.04\ s^{-1}$
$k_{-3} = 32.0\ s^{-1}$
$k_5 = 1.0\ s^{-1}$
$k_{-5} = 0.14\ s^{-1}$
$k_{43} = 0.1\ s^{-1}$
$k_{34} = 0.14\ s^{-1}$

$k_1 = 3.95\ s^{-1}$
$k_{-1} = 8.13\ s^{-1}$
$k_2 = 36.05\ s^{-1}$
$k_{-2} = 2.13\ s^{-1}$
$k_3 = 0.14\ s^{-1}$
$k_{-3} = 50.0\ s^{-1}$

types of channel activity are distinguishable by the presence of slow voltage-dependent inactivation; and (*c*) inactivation of the DHP-sensitive calcium channel observed at the single-channel level may contribute to the decay of I_{Ca} recorded at the cellular level.

The authors are deeply grateful to Dr. J. García for his help in the cut fiber experiments; to Drs. R. Latorre, O. Alvarez, A. M. Brown, and A. M. J. VanDongen for analysis software; to Dr. S. L. Hamilton for binding measurements; and to Mr. Garland Cantrell for building the bilayer amplifier.

This work was supported by a National Institutes of Health grant (R01 AR-38970) to E. Stefani and by a MDA postdoctoral fellowship to M. Fill.

Original version received 4 December 1989 and accepted version received 13 August 1990.

REFERENCES

Almers, W., R. Fink, and P. T. Palade. 1981. Calcium depletion in frog muscle tubules: the decline of calcium current under maintained depolarization. *Journal of Physiology.* 312:177–207.

Armstrong, C. M., F. Bezanilla, and E. Rojas. 1973. Destruction of sodium conductance inactivation in squid axon perfused with pronase. *Journal of General Physiology.* 62:375–391.

Beaty, G. N., and E. Stefani. 1976. Inward calcium current in twitch muscle fibres of the frog. *Journal of Physiology.* 260:27P. (Abstr.)

Blatz, A. L., and K. L. Magleby. 1989. Adjacent interval analysis distinguishes among gating mechanisms for the fast chloride channel from rat skeletal muscle. *Journal of Physiology.* 410:561–585.

Brehm, P., and R. Eckert. 1978. Calcium entry leads to inactivation of calcium channel in *Paramecium. Science.* 202:1203–1206.

Brown, A. M., H. Camerer, D. L. Kunze, and H. D. Lux. 1982. Similarity of unitary Ca^{2+} currents in three different species. *Nature.* 299:156–158.

Chiarandini, D. J., and E. Stefani. 1983. Calcium action potentials in rat fast-twitch and slow-twitch muscle fibers. *Journal of Physiology.* 335:29–40.

Colquhoun, D., and A. G. Hawkes. 1982. On the stochastic properties of bursts of single ion channel opening and of clusters of bursts. *Philosophical Transactions of the Royal Society of London, B Biological Sciences.* 300:1–59.

Colquhoun, D., and F. J. Sigworth. 1983. Fitting and statistical analysis of single-channel records. *In* Single Channel Recording. B. Sakmann, and E. Neher, editors. Plenum Publishing Corp., New York. 191–263.

Coronado, R., and H. Affolter. 1986. Characterization of dihydropyridine sensitive calcium channels from purified skeletal muscle transverse tubules. *In* Ion Channel Reconstitution. C. Miller, editor. Plenum Publishing Corp., New York. 483–505.

Cota, G., L. Nicola-Siri, and E. Stefani. 1984. Calcium channel inactivation in frog (*Rana pipiens* and *Rana moctezuma*) skeletal muscle fibres. *Journal of Physiology.* 354:99–108.

Cota, G., and E. Stefani. 1984. Saturation of calcium channels and surface charge effects in skeletal muscle fibres of the frog. *Journal of Physiology.* 351:135–154.

Cota, G., and E. Stefani. 1986. A fast-activated inward calcium current in twitch muscle fibres of the frog (*Rana montezume*). *Journal of Physiology.* 370:151–163.

Cota, G., and E. Stefani. 1989. Voltage-dependent inactivation of slow calcium channels in intact twitch muscle fibers of the frog. *Journal of General Physiology.* 94:937–951.

Donaldson, P. L., and K. G. Beam. 1983. Calcium currents in a fast-twitch skeletal muscle of the rat. *Journal of General Physiology.* 82:449–468.

Fenwick, E. M., A. Marty, and E. Neher. 1982. Sodium and calcium channels in bovine chromaffin cells. *Journal of Physiology.* 331:599–635.

Francini, F., and E. Stefani. 1989. The decay of the slow calcium current in twitch muscles fibers of the frog is influenced by intracellular EGTA. *Journal of General Physiology.* 94:953–969.

García, J., R. Gamboa-Aldeco, and E. Stefani. 1988. Two types of calcium currents in mammalian skeletal muscle. *Society for Neurosciences Abstracts.* 14:140*a*. (Abstr.)

García, J., and E. Stefani. 1987. Appropriate conditions to record activation of fast Ca^{2+} channels in frog skeletal muscle (*Rana pipiens*). *Pflügers Archiv.* 408:646–648.

Hamilton, S. L., R. Mejía-Alvarez, M. Fill, M. J. Hawkes, K. Brush, W. P. Schilling, and E. Stefani. 1989. [^{3}H]PN200-110 and [^{3}H]ryanodine binding and reconstitution of ion channel activity with skeletal muscle membranes. *Analytical Biochemistry.* 183:31–41.

Hess, P., J. B. Lansman, and R. W. Tsien. 1984. Different modes of Ca^{2+} channel gating behavior favored by dihydropyridine Ca^{2+} agonist and antagonists. *Nature.* 311:538–544.

Hodgkin, A. L., and A. F. Huxley. 1952. A quantitative description of membrane current and its application to conduction and excitation in nerve. *Journal of Physiology.* 117:500–544.

Irving, M., J. Maylie, N. L. Sizto, and W. K. Chandler. 1987. Intrinsic optical and passive electrical properties of cut frog twitch fibers. *Journal of General Physiology.* 89:1–40.

Kovács, L., E. Ríos, and M. F. Schneider. 1983. Measurements and modification of free calcium transients in frog skeletal muscle fibers by a metallochromic indicator dye. *Journal of Physiology.* 343:161–196.

Lacerda, A. E., and A. M. Brown. 1989. Nonmodal gating of cardiac calcium channels as revealed by dihydropyridines. *Journal of General Physiology.* 93:1243–1273.

Lamb, G. D., and T. Walsh. 1987. Calcium currents, charge movement and dihydropyridine binding in fast and slow-twitch muscles of rat and rabbit. *Journal of Physiology.* 393:595–617.

Ma, J., and R. Coronado. 1988. Heterogeneity of conductance states in calcium channels of skeletal muscle. *Biophysical Journal.* 53:387–395.

Nicola-Siri, L., J. A. Sánchez, and E. Stefani. 1980. Effect of glycerol treatment on the calcium current of frog skeletal muscle. *Journal of Physiology.* 305:87–96.

Rosenberg, R. L., P. Hess, and R. W. Tsien. 1988. Cardiac calcium channels in planar lipid bilayers. *Journal of General Physiology.* 92:27–54.

Sánchez, J. A., and E. Stefani. 1983. Kinetic properties of calcium channels of twitch muscle fibres of the frog. *Journal of Physiology.* 337:1–17.

Sanguinetti, M. C., D. S. Krafte, and R. S. Kass. 1986. Voltage-dependent modulation of Ca^{2+} channel current in heart cells by Bay K 8644. *Journal of General Physiology.* 88:369–392.

Sigworth, F. J., and S. M. Sine. 1987. Data transformations for improved display and fitting of single-channel dwell time histograms. *Biophysical Journal.* 52:1047–1054.

Stanfield, P. R. 1977. A calcium dependent inward current in frog skeletal muscle fibres. *Pflügers Archiv.* 368:267–270.

Tillotson, D. 1979. Inactivation of Ca conductance dependent on entry of Ca ions in molluscan neurons. *Proceedings of the National Academy of Sciences USA.* 76–3:1497–1500.

Yatani, A., Y. Imoto, J. Codina, S. L. Hamilton, A. M. Brown, and L. Birnbaumer. 1988. The stimulatory G protein of adenylyl cyclase, G_s, also stimulates dihydropyridine-sensitive Ca^{2+} channels. *Journal of Biological Chemistry.* 263:9887–9895.